The effects of plasticity on the convergence of iterative solvers

A. Ramage[c,*], P.G. Smith[c], C.E. Augarde[a], A.M. Sonnet[c], C. Matthews[b]

[a]School of Engineering and Computing Sciences, Durham University, Durham DH1 3LE.
[b]Oasys Ltd, Central Square, Forth Street, Newcastle-upon-Tyne NE1 3PL.
[c]Department of Mathematics and Statistics, University of Strathclyde, Glasgow G1 1XH.

Abstract

In geotechnical finite element analysis, iterative solvers are generally preferred to direct solvers, and for larger problems iterative solvers usually provide the only economical way for calculating solutions on a desktop PC. In practice, the speed of convergence of an iterative solver can be increased significantly by using a suitable preconditioner. However, the wide range of elasto-plastic constitutive models and the changing nature of the equations during the analysis make effective preconditioning particularly difficult in geotechnical FE analysis. Knowledge of the eigenvalue spectrum of the stiffness matrix is helpful in designing effective preconditioners. In this paper we look at the eigenvalues of the element stiffness matrix when elasto-plastic models such as the Mohr-Coulomb model are used. Specifically, we consider the effect on the condition number from the onset of plasticity. This should provide valuable insight for constructing effective preconditioners for elasto-plastic problems.

Keywords:

1. Background

Finite element (FE) techniques are widely used in geotechnical engineering for modelling many situations of practical interest. As the scope and complexity of the models being studied grows, so does the need for efficient numerical algorithms to ensure that the problems can be solved using a realistic amount of computational time and computer memory. A typical FE analysis usually involves linearisation within a nonlinear iteration procedure, such as a modified Euler or Newton-Raphson methods (see, for example, [1, 2]). With these approaches, each nonlinear iteration involves a large, sparse linear system of the form

$$\mathbf{K}\mathbf{u} = \mathbf{f} \tag{1}$$

(where $\mathbf{K}$ is the structure stiffness matrix and $\mathbf{f}$ represents the load vector) which must be solved for the nodal displacements $\mathbf{u}$. For many realistic problems, the use of direct methods such as Gaussian Elimination to solve (1) is simply not practical, hence there is a pressing need to develop efficient iterative methods to do this.

For problems where the coefficient matrix $\mathbf{K}$ is symmetric and positive definite (SPD), the method of choice is usually the conjugate gradient (CG) method [3]. The convergence behaviour of CG is well understood and is known to depend on the eigenvalue spectrum of $\mathbf{K}$. This suggests the idea of *preconditioning* system (1): theoretically, this is equivalent to replacing $\mathbf{K}$ by a preconditioned matrix $\mathbf{P}^{-1}\mathbf{K}$ whose eigenvalue spectrum facilitates faster CG convergence, leading to the Preconditioned Conjugate Gradient (PCG) method [4]. In particular, it can be shown that the number of PCG iterations required for convergence to within a specified tolerance is proportional to the square root of the condition number $\kappa = \lambda_{\max}/\lambda_{\min}$, where $\lambda_{\max}$ and $\lambda_{\min}$ are the extreme eigenvalues of the preconditioned coefficient matrix (see, for example, [5]). One preconditioning strategy is therefore to find a preconditioner $\mathbf{P}$ such that the condition number of $\mathbf{P}^{-1}\mathbf{K}$ is smaller than that of $\mathbf{K}$. However, this must be done whilst ensuring that the action of the matrix $\mathbf{P}^{-1}$ (required by the PCG algorithm) is available at a reasonable cost.

The development of efficient preconditioners is a vibrant area of current research (see e.g. [6]). Although PCG methods have been used successfully for structural engineering problems such as linear elasticity [7, 8, 9, 10, 11], the issues surrounding preconditioning problems in other geotechnical finite element analyses are less well understood, particularly when the coefficient matrix in (1) is not SPD (see, for example, [12, 13]). For nonsymmetric systems, preconditioned versions of alternative iterative methods such as GMRES [14], Bi-CGSTAB [15] or IDR(s) [16] must be used. Although convergence properties for these methods are not as well understood as for PCG, it is generally accepted that in many cases, the eigenvalue spectrum still plays an important role. In this paper, we will consider some model problems with elasto-plastic material behaviour, leading to a nonsymmetric $\mathbf{K}$ at the onset of plasticity, and make some observations about the eigenvalues of $\mathbf{K}$ which should be helpful in the design of preconditioners for nonsymmetric iterative algorithms.

*Corresponding author
Email address: A.Ramage@strath.ac.uk (A. Ramage)

2. Outline of the finite element model

As an illustration, we consider a problem discretised using a total of N_{dof} degrees of freedom on a domain Ω^d in d dimensions, with N_E finite elements whose nodes do not have rotational freedoms. For an element with N_e nodes, the element stiffness matrix can be constructed by evaluating the integral

$$\mathbf{K}_e = \int_V \mathbf{B}^T \mathbf{D} \mathbf{B} \, dV \tag{2}$$

over the element length, area or volume. Here $\mathbf{B}$ is a $6 \times dN_e$ matrix containing derivatives of the shape functions and $\mathbf{D}$ is a 6×6 matrix expressing the constitutive behaviour of the material (see, for example, [17, §2.6]), so that $\mathbf{K}_e$ is of size $dN_e \times dN_e$. The global coefficient matrix $\mathbf{K}$ in (1) can then be constructed using an $dN_e \times N_{dof}$ Boolean connectivity matrix $\mathbf{C}_e$ via the steps

$$\bar{\mathbf{K}}_\mathbf{e} = \mathbf{C}_e^T \mathbf{K}_e \mathbf{C}_e \text{ for } e = 1, \ldots, N_E, \qquad \mathbf{K} = \sum_{e=1}^{N_E} \bar{\mathbf{K}}_\mathbf{e}.$$

When the assembled stiffness matrix $\mathbf{K}$ is symmetric, bounds on its extreme eigenvalues can be obtained by considering the eigenvalues of individual element matrices. Specifically, it is shown in [18] that

$$\min_e \lambda_{\min}(\mathbf{K}_e) \quad \leq \lambda(\mathbf{K}) \leq \quad \max_e \lambda_{\max}(\mathbf{K}_e) \tag{3}$$

where $\lambda_{\min}(\mathbf{K}_e)$ and $\lambda_{\max}(\mathbf{K}_e)$ represent the extreme eigenvalues of the element matrix $\mathbf{K}_e$. Although the left-hand inequality can essentially be disregarded here (as it simply gives a lower bound of zero), the right-hand inequality can be used to predict the dependence of the maximum eigenvalue on problem parameters. Note that if an element-based preconditioner $\mathbf{P}$ is assembled in an analogous way, result (3) also applies to the preconditioned system. To our knowledge, (3) has not been extended to include nonsymmetric problems, but we anticipate that this may be possible, at least for the subclass of nonsymmetric matrices whose eigenvalues are real. The fact that the nonsymmetric matrices produced by nonassociated plasticity have real eigenvalues is certainly true for the Mohr-Coulomb examples studied in this paper, and has been shown more generally for a Drucker-Prager model in [19]. With this in mind, in this paper we study properties of the maximum eigenvalue of element matrices of the form (2) with a view to investigating their dependence on material properties.

3. Constitutive behaviour for elasto-plastic problems

For a linear elastic material, the matrix $\mathbf{D}$ in (2) takes the form

$$\mathbf{D^{el}} = \frac{E}{(1-2\nu)(1+\nu)} \begin{bmatrix} 1-\nu & \nu & \nu & 0 & 0 & 0 \\ \nu & 1-\nu & \nu & 0 & 0 & 0 \\ \nu & \nu & 1-\nu & 0 & 0 & 0 \\ 0 & 0 & 0 & \frac{1}{2}-\nu & 0 & 0 \\ 0 & 0 & 0 & 0 & \frac{1}{2}-\nu & 0 \\ 0 & 0 & 0 & 0 & 0 & \frac{1}{2}-\nu \end{bmatrix} \tag{4}$$

where E is Young's modulus and ν is Poisson's ratio (see, for example, [17]). Representing the stresses and strains (normal and shear) in vector form as

$$\boldsymbol{\sigma} = [\sigma_x, \sigma_y, \sigma_z, \tau_{xy}, \tau_{yz}, \tau_{xz}]^T, \qquad \boldsymbol{\epsilon} = [\epsilon_x, \epsilon_y, \epsilon_z, \gamma_{xy}, \gamma_{yz}, \gamma_{xz}]^T,$$

the linear elastic relationship between the stress and strain rates can be written as $\dot{\boldsymbol{\sigma}} = \mathbf{D^{el}} \dot{\boldsymbol{\epsilon}}$. For an elasto-plastic constitutive model under small deformations with yield function $F(\boldsymbol{\sigma})$ and plastic potential function $P(\boldsymbol{\sigma})$, it can be shown that the analogous relationship $\dot{\boldsymbol{\sigma}} = \mathbf{D^{ep}} \dot{\boldsymbol{\epsilon}}$ holds, where (for perfect plasticity) the constitutive matrix takes the form

$$\mathbf{D^{ep}} = \mathbf{D^{el}} - \frac{\mathbf{D^{el}} \left(\dfrac{\partial P}{\partial \boldsymbol{\sigma}} \right) \left(\dfrac{\partial F}{\partial \boldsymbol{\sigma}} \right)^T \mathbf{D^{el}}}{\left(\dfrac{\partial F}{\partial \boldsymbol{\sigma}} \right)^T \mathbf{D^{el}} \left(\dfrac{\partial P}{\partial \boldsymbol{\sigma}} \right)}. \tag{5}$$

(see, for example, [20]). Different forms of the yield and plastic potential functions will clearly lead to different matrices $\mathbf{D^{ep}}$. For associated flow (that is, when $F \equiv P$), $\mathbf{D^{ep}}$ will be symmetric: otherwise, $\mathbf{D^{ep}}$ will be nonsymmetric. We observe that, in linear algebra terminology, $\mathbf{D^{ep}}$ is simply a rank-one update of $\mathbf{D^{el}}$.

4. Two Mohr-Coulomb model problems

Assuming the principal stresses σ_1, σ_2 and σ_3 are such that $\sigma_1 \geq \sigma_2 \geq \sigma_3$, for a Mohr-Coulomb model the onset of plastic deformation is controlled by the yield function

$$\sigma_1(1 - \sin\theta) - \sigma_3(1 + \sin\theta) = 2c\cos\theta \tag{6}$$

where c is the cohesion of the material and θ is the angle of internal friction (see, for example, [20]). The plastic potential function is taken to be

$$\sigma_1(1 - \sin\psi) - \sigma_3(1 + \sin\psi) = 2c\cos\psi \tag{7}$$

where ψ is the angle of dilation for the material. Taking $\psi = \theta$ (associated flow) leads to a symmetric model but otherwise, after the onset of plasticity, some of the element matrices in (2) (and hence the coefficient matrix in (1)) will be nonsymmetric. We now examine the use of this model in two different settings.

Homogeneous 2D plane strain with applied normal tractions
Here we consider a block of cohesionless sand loaded in plane strain conditions with applied normal tractions along all four edges [20, §3.8]. The coordinate axes are chosen along the principal directions, with no extensional strain in the z-direction. The stress matrix is therefore diagonal, and the principal stresses are σ_x, σ_y and σ_z. If the block is initially unstressed then stresses σ_x and σ_y are increased (equally) to a value of p_0, the principal stresses are given by $\sigma_x = \sigma_y = p_0$ and $\sigma_z = 2\nu p_0$. In this case, the linear elastic constitutive matrix (4) simplifies to

$$\mathbf{D}^{\mathbf{el}} = \frac{E}{(1+\nu)(1-2\nu)} \begin{bmatrix} 1-\nu & \nu \\ \nu & 1-\nu \end{bmatrix}, \tag{8}$$

which has maximum eigenvalue

$$\lambda_{\max}(\mathbf{D}^{\mathbf{el}}) = \frac{E}{(1+\nu)(1-2\nu)}. \tag{9}$$

In a similar way, (5) evaluates to

$$\mathbf{D}^{\mathbf{ep}} = \frac{E}{2(1+\nu)(1-2\nu+\sin\theta\sin\psi)} \begin{bmatrix} (1-\sin\theta)(1-\sin\psi) & (1+\sin\theta)(1-\sin\psi) \\ (1+\sin\psi)(1-\sin\theta) & (1+\sin\theta)(1+\sin\psi) \end{bmatrix} \tag{10}$$

(see [20, p. 99]). This matrix has only one nonzero eigenvalue, given by

$$\lambda_{\max}(\mathbf{D}^{\mathbf{ep}}) = \frac{E(1+\sin\theta\sin\psi)}{(1+\nu)(1-2\nu+\sin\theta\sin\psi)}. \tag{11}$$

Using a finite element model with bilinear basis functions on square elements of side length h (that is, with four nodes per element), the 8×8 element stiffness matrix for elastic elements (using (8)) can be shown to be of the form

$$\mathbf{K}_e^{\mathbf{el}} = \frac{E}{(1+\nu)(1-2\nu)} \begin{bmatrix} \frac{1}{6}(1-\nu)\,A_1 & \frac{1}{4}\nu\,A_2 \\ \frac{1}{4}\nu\,A_2^T & \frac{1}{6}(1-\nu)\,A_3 \end{bmatrix} \tag{12}$$

where

$$A_1 = \begin{bmatrix} 2 & -2 & -1 & 1 \\ -2 & 2 & 1 & -1 \\ -1 & 1 & 2 & -2 \\ 1 & -1 & -2 & 2 \end{bmatrix}, \quad A_2 = \begin{bmatrix} 1 & 1 & -1 & -1 \\ -1 & -1 & 1 & 1 \\ -1 & -1 & 1 & 1 \\ 1 & 1 & -1 & -1 \end{bmatrix}, \quad A_3 = \begin{bmatrix} 2 & 1 & -1 & -2 \\ 1 & 2 & -2 & -1 \\ -1 & -2 & 2 & 1 \\ -2 & -1 & 1 & 2 \end{bmatrix}. \tag{13}$$

The maximum eigenvalue of $\mathbf{K}_e^{\mathbf{el}}$ is the same as that of $\mathbf{D}^{\mathbf{el}}$ (as given in (9)). Note that this eigenvalue (and hence the condition number) tends to infinity as $\nu \to 0.5$, indicating a potential problem for iterative convergence.

In a similar way, the equivalent elasto-plastic finite element stiffness matrix (constructed using (5)) can be written as

$$\mathbf{K}_e^{\mathbf{ep}} = \frac{E}{2(1+\nu)(1-2\nu+\sin\theta\sin\psi)} \begin{bmatrix} \frac{1}{6}(1-\sin\theta)(1-\sin\psi)\,A_1 & \frac{1}{4}(1+\sin\theta)(1-\sin\psi)\,A_2 \\ \frac{1}{4}(1-\sin\theta)(1+\sin\psi)\,A_2^T & \frac{1}{6}(1+\sin\theta)(1+\sin\psi)\,A_3 \end{bmatrix} \tag{14}$$

again using the matrices in (13). The maximum eigenvalue of (14) is the same as that of $\mathbf{D}^{\mathbf{ep}}$ (as given in (11)). In contrast to the elastic case, the denominator of this eigenvalue is bounded away from 0 for non-zero θ, ϕ as $\nu \to 0.5$.

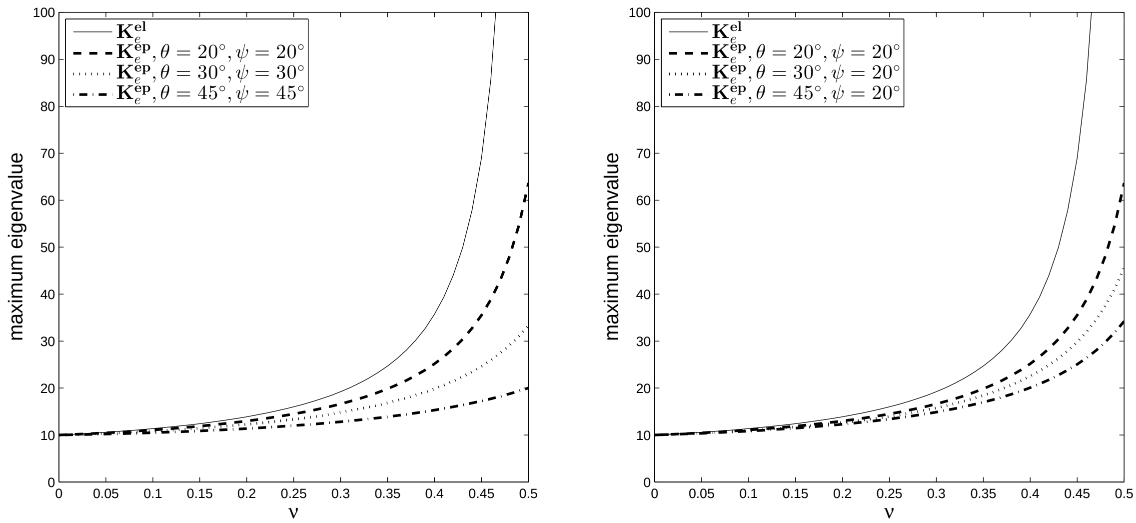

Figure 1: Comparison of $\lambda_{\max}(K_e)$ for the elastic and elasto-plastic cases with two-dimensional homogeneous plane strain.

Comparing (11) with (9), we see that, when $\nu = 0$, the maximum eigenvalues both equal E. As $\nu \to 0.5$, however, the former is bounded above by

$$\frac{2E}{3}\left(1 + \frac{1}{\sin\theta \sin\psi}\right)$$

whereas the latter is unbounded. This effect is illustrated in Figure 1 for Young's modulus $E = 10$. We note that in practice, the value of θ (the angle of internal friction) typically lies in the range 20° to 45°: the results shown here are for representative values in this range. In the left-hand plot, $\theta = \psi$ in each case so the flow is associated and the matrices symmetric. The right-hand plot show results for an example with $\theta \neq \psi$ (non-associated flow). The eigenvalue behaviour is similar for other realistic combinations of θ and ψ.

Homogeneous 3D plane strain with applied normal tractions

We now carry out an equivalent analysis for the analogous homogeneous plane strain problem in a three-dimensional box. Here the linear elastic constitutive matrix (4) is the 3×3 matrix to

$$\mathbf{D}^{\mathbf{el}} = \frac{E}{(1+\nu)(1-2\nu)} \begin{bmatrix} 1-\nu & \nu & \nu \\ \nu & 1-\nu & \nu \\ \nu & \nu & 1-\nu \end{bmatrix}, \tag{15}$$

which has maximum eigenvalue

$$\lambda_{\max}(\mathbf{D}^{\mathbf{el}}) = \frac{E}{1-2\nu}. \tag{16}$$

Discretising with eight-node trilinear box elements of side length h, it can be shown that the associated element matrix has maximum eigenvalue

$$\lambda_{\max}(\mathbf{K}_e^{\mathbf{el}}) = \frac{h}{2}\lambda_{\max}(\mathbf{D}^{\mathbf{el}}).$$

In [21], Yu derives the elasto-plastic constitutive matrix of a Mohr-Coulomb model for two different examples of stress state. In the case where the stress state lies at the corner defined by two individual yield functions, he gives the elasto-plastic constitutive matrix as

$$\mathbf{D}^{\mathbf{ep}} = C \begin{bmatrix} (1+\sin\theta)(1+\sin\psi) & (1+\sin\theta)(1-\sin\psi) & (1+\sin\theta)(1-\sin\psi) \\ (1-\sin\theta)(1+\sin\psi) & (1-\sin\theta)(1-\sin\psi) & (1-\sin\theta)(1-\sin\psi) \\ (1-\sin\theta)(1+\sin\psi) & (1-\sin\theta)(1-\sin\psi) & (1-\sin\theta)(1-\sin\psi) \end{bmatrix}$$

where

$$C = \frac{3E}{8(1+\nu)\sin\psi\sin\theta + (1-2\nu)(3-\sin\psi)(3-\sin\theta)}.$$

This matrix has maximum eigenvalue

$$\lambda_{\max}(\mathbf{D}^{\mathbf{ep}}) = \frac{3E(3(1+\sin\theta\sin\psi) - (\sin\theta + \sin\psi))}{8(1+\nu)\sin\psi\sin\theta + (1-2\nu)(3-\sin\psi)(3-\sin\theta)} \tag{17}$$

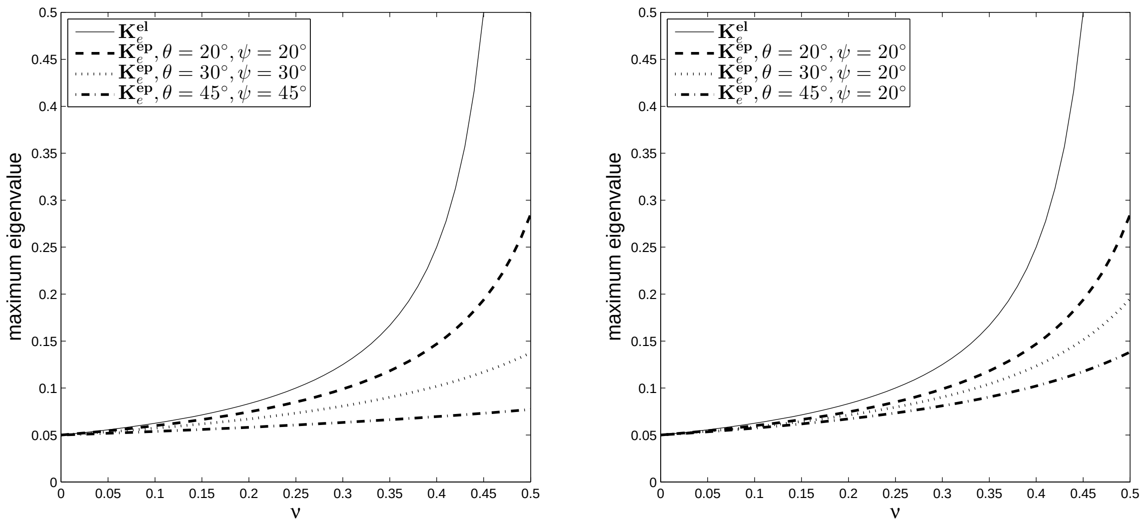

Figure 2: Comparison of $\lambda_{\max}(K_e)$ for the elastic and elasto-plastic cases with three-dimensional homogeous plane strain.

and, as in the elastic case, the maximum eigenvalue of the full elasto-plastic element matrix is a simple scaling of this, namely

$$\lambda_{\max}(\mathbf{K}_e^{\mathbf{ep}}) = \frac{h}{2}\lambda_{\max}(\mathbf{D}^{\mathbf{ep}}).$$

Comparing $\lambda_{\max}(\mathbf{K}_e^{\mathbf{el}})$ and $\lambda_{\max}(\mathbf{K}_e^{\mathbf{ep}})$ in this case, we see that when $\nu = 0$, they are both equal to $hE/2$. However, as in the two-dimensional case, in the limit as $\nu \to 0.5$, $\lambda_{\max}(\mathbf{K}_e^{\mathbf{ep}})$ is bounded above, by

$$\frac{hE(3(1 + \sin\theta\sin\psi) - (\sin\theta + \sin\psi))}{4\sin\theta\sin\psi},$$

whereas $\lambda_{\max}(\mathbf{K}_e^{\mathbf{el}})$ grows in an unbounded way.

Figure 2 shows the analogous plots to Figure 1 for the three-dimensional case, again for $E = 10$, with $h = 0.01$. The plots show very similar behaviour to the two-dimensional case.

5. Summary

It is well known that the convergence rate of a Krylov-subspace iterative method is usually adversely affected by growth in the condition number of the coefficient matrix. In this paper, we have illustrated why iterative solution of linear elastic problems is difficult, as we have seen unbounded growth in the largest eigenvalue of the linear elastic element matrix in the limit as Poisson's ratio $\nu \to 0.5$. In contrast, for a Mohr-Coulomb model of plane strain perfect plasticity, the maximum eigenvalue of the element stiffness matrix is bounded above by a constant (dependent on the angle of internal friction θ and the angle of dilation ψ) as ν grows. This hold for both associated (symmetric) and non-associated (non-symmetric) flow problems. Our conclusion is therefore that when designing preconditioners for elasto-plastic problems, the key issue is how to precondition the elastic part of $\mathbf{K}$, as this will dominate the overall eigenvalue structure.

References

[1] E. Hairer, G. Wanner, Solving Ordinary Differential Equations II: Stiff and Differential-Algebraic Problems, Springer Series in Computational Mathematics, Springer, 2010.

[2] T. Kelley, Iterative Methods for Linear and Nonlinear Equations, SIAM, Philadelphia, 1995.

[3] M. R. Hestenes, E. Stiefel, Methods of conjugate gradients for solving linear systems, Journal of Research of the National Bureau of Standards 49 (1952) 409–436.

[4] P. Concus, G. H. Golub, D. P. O'Leary, A generalized conjugate gradient method for the numerical solution of elliptic partial differential equations, in: J. R. Bunch, D. J. Rose (Eds.), Sparse Matrix Computations, Academic Press, NY, 1976, pp. 309–332.

[5] O. Axelsson, V. A. Barker, Finite element solution of boundary value problems, SIAM, 2001.

[6] M. Benzi, Preconditioning techniques for large linear systems: A survey, Journal of Computational Physics 182 (2002) 418–477.

[7] C. E. Augarde, A. Ramage, J. Staudacher, On element-based preconditioners for linear elasticity problems, Computers and Structures 84 (2006) 2306–2315.

[8] J. K. Dickinson, P. A. Forsyth, Preconditioned conjugate gradient methods for three-dimensional linear elasticity, International Journal for Numerical Methods in Engineering 37 (1994) 2211–2234.

[9] E. Graham, P. A. Forsyth, Preconditioning methods for very ill-conditioned three-dimensional linear elasticity problems, International Journal for Numerical Methods in Engineering 44 (1999) 77–99.

[10] I. Hladik, M. B. Reed, G. Swoboda, Robust preconditioners for linear elasticity FEM analyses, International Journal for Numerical Methods in Engineering 40 (1997) 2109–2127.

[11] P. Saint-Georges, G. Warzee, R. Beauwens, Y. Notay, High-performance PCG solvers for FEM structural analysis, International Journal for Numerical Methods in Engineering 39 (1996) 1313–1340.

[12] C. E. Augarde, A. Ramage, J. Staudacher, Element-based preconditioners for elasto-plastic problems in geotechnical engineering, International Journal for Numerical Methods in Engineering 71 (2007) 757–882.

[13] H. Mroueh, I. Shahrour, Use of sparse iterative methods for the resolution of three-dimensional soil/structure interaction problems, International Journal for Numerical and Analytical Methods in Geomechanics 23 (1999) 1961–1975.

[14] Y. Saad, M. H. Schultz, GMRES: a Generalized Minimal Residual algorithm for solving nonsymmetric linear systems, SIAM Journal on Scientific and Statistical Computing 7 (1986) 856–869.

[15] H. A. van der Vorst, Bi-CGSTAB: A fast and smoothly converging variant of Bi-CG for the solution of nonsymmetric linear systems, SIAM Journal on Scientific and Statistical Computing 13 (1992) 631–644.

[16] M. B. van Gijzen, P. Sonneveld, Algorithm 913: An elegant IDR(s) variant that efficiently exploits bi-orthogonality properties, ACM Transactions on Mathematical Software 38 (2011) 1–19.

[17] D. M. Potts, L. Zdravković, Finite Element Analysis in Geotechnical Engineering: Theory, Thomas Telford, 1999.

[18] A. J. Wathen, Spectral bounds and preconditioning methods using element-by-element analysis for Galerkin finite element equations, in: J. R. Whiteman (Ed.), The Mathematics of Finite Elements and Applications VI (MAFELAP 1987), Academic Press, 1988, pp. 157–168.

[19] H. van der Veen, C. Vuik, R. de Borst, An eigenvalue analysis of nonassociated plasticity, Computers and Matheamtocs with Applications 38 (1999) 107–115.

[20] R. O. Davis, A. P. S. Selvadurai, Plasticity and Geomechanics, Cambridge University Press, 2005.

[21] H. S. Yu, A closed-form solution of the stiffness matrix for Tresca and Mohr-Coulomb plasticity models, Computers and Structures 53 (1994) 755–757.